Effect of Salty Fog on Flashover Characteristics of OCS Composite Insulators*

Sihua Wang [1,2*] *and Youlong Wu* [1,2]

(1. College of Automation & Electrical Engineering, Lanzhou Jiaotong University, Lanzhou 730070, China;
2. Rail Transit Electrical Automation Engineering Laboratory of Gansu Province,
Lanzhou Jiaotong University, Lanzhou 730070, China)

Abstract: To study the flashover characteristics of the fog water in saline-alkali areas for high-speed railway OSC insulators, the spatial distributions of both the potential and electric field of soiled insulators in the presence of salty fog are analyzed using COMSOL Multiphysics, a multi-physics coupling software. Furthermore, to analyze the effect of the contamination of insulators due to salty fog water , a saline solution is used for staining an insulator sample by using the solid coating method. In an artificial climate chamber, the salty fog environment is simulated, and the flashover voltage for different salty fog water conductivities and surface staining are obtained. The salt-density correction coefficient K is also proposed. It provides a strong basis for the selection of railway insulators in saline-alkali areas. The results show that the salty fog water changes the original surface equivalent salt density, ρESDD, by wetting the existing fouling layer on the surface of the insulator, so that the original surface contamination layer becomes equivalent to $K\rho_{ESDD}$; the smaller is the value of ρ_{ESDD} of the insulator surface, the larger is the value of K; the surface of the same insulator is dirty, and as the concentration of salty fog-water increases, K also increases.

Keywords: Salty fog; composite insulators; flashover characteristics; COMSOL multiphysics; additional salt density

1 Introduction

The Lanxin line (Lanzhou--Autonomous Region, Xinjiang) is located in the north-western part of China. The salinization of the land along this line is a very serious issue. According to an investigation, the Lanxin line passes through several salt lakes, and the saline-alkali particles in the environment easily to adhere to the surface of the railway insulators, especially around the salt lakes. Furthermore, the high-conductivity salty fog causes frequent flashover accidents when the salt-lake environment comes in contact with grid insulators.

The effect of insulator surface area fouling on hydrophobicity has been studied in the Refs. [1-3]. The results showed that the hydrophobic migration rate of the surface of silicone rubber will decrease after staining. The insulator's flashover voltage in high-conductivity fog was also studied in the Refs. [4-5], and the results showed that high-conductivity fog greatly influences the flashover voltage. The flashover characteristics of suspended porcelain insulators in high-conductivity fog were also studied [6]. The results showed that the flashover voltage of short-chain porcelain insulators decreases upon increase in the conductivity of fog water, but long-chain composite insulators were not studied. The flashover characteristics of grid insulators for silicon rubber materials under charged salt spray environment were also studied [7]. It was concluded that the flashover voltage of the insulator sample was related to the charged voltage value. The higher the voltage value applied during the charging test, the sooner the charging test ended. On decreasing the flashover voltage, a more negative-power exponential relationship was observed between the flashover voltage and the fog-water conductivity. Furthermore, the Refs. [8-10] indicate the threshold of the conductivity of natural fog water in China (the maximum conductivity of fog in some areas can reach 0.619 S/m); high conductivity fog will pose a serious threat to the transmission line.

Although domestic and foreign scholars have conducted a lot of research on the alternating flashover characteristics of contaminated insulators, yet the research regarding the influence of the special high-conductivity salty fog on the AC flashover characteristics of composite insulators is scarce and

* Corresponding Author, Email: 643374980@qq.com
* Supported by the Natural Science Foundation of China(51567014, 51767014) and the Scientific and Technological Research and Development Program of the China Railway (2017J010-C/2017)
Digital Object Identifier: 10.23919/CJEE.2019.000021

lacks test data and precise conclusions.

With a view to studying the effect of the salty fog environment on the railway-specific FQBG-25 wrist arm insulators, the artificial contamination test under different salty fog conductivities was performed to analyze the influence of both salt density and conductivity of salty fog water on the AC characteristics of contaminated silicone rubber composite insulators. To that end, the COMSOL Multiphysics simulation software was used to calculate the potential and the electric field of the full-size insulator, following which the spatial distributions of both potential and electric field of the insulator in the salty fog were obtained under different fog-water conductivity values.

2 Test facilities, samples, and test procedures

2.1 Test facilities

The experiment was performed in an artificial climate chamber at the high-voltage laboratory of Lanzhou Jiaotong University. The dimension of the climate chamber was 1.2 mm×1.2 mm×1.8 mm. Inside the chamber, the indoor-temperature adjustment range was －20-40℃, and the fog was generated via ultrasonic fogging. The device and wiring schematic are depicted in Fig. 1. The AC pollution test transformer used in this experiment has the rated voltage of 50 kV, rated current of 1 A, and a protective resistance value of 0.8 kΩ, all of which meet the requirements of the national standard GB/T 4585-2004 for the AC pollution test power supply. The test power source was introduced into the artificial climate chamber by using a high-voltage wall bushing. The ultrasonic water mist generator (YC-G030T) produced mist water with an average particle size of 1 μm to 10μm. By the sampling and analysis of several salt lakes, the calculation formula provided in the Ref. [11] can be obtained. The conductivity of salty fog water, σ, ranged from 0.08 S/m to 0.45 S/m, and the test was prepared for five fog water cases each with conductivity of 0.002 S/m (clean mist), 0.01 S/m, 0.10 S/m, 0.30 S/m, and 0.50 S/m, respectively.

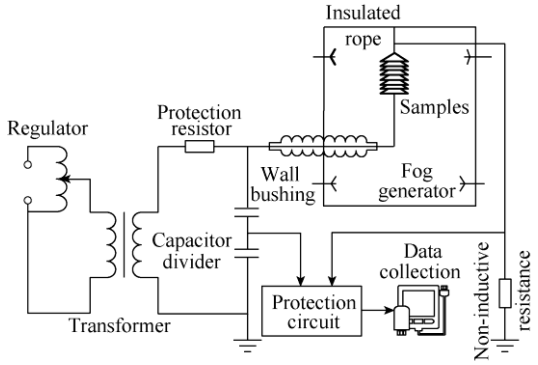

Fig. 1 Wiring diagram of the test

2.2 Test samples

The test product used was the FQBG-25 railway composite insulator, which was provided by Urumqi Railway Group Corporation and was consistent with the composite insulator used in the special section of the salty fog. The structure diagram of the composite insulator is depicted in Fig. 2. A prepared contaminated solution was quantitatively and uniformly applied to the surface of the insulator by using solid coating method.

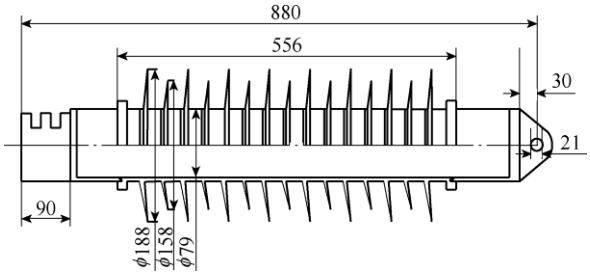

Fig. 2 Insulator's structure diagram

The distribution of the contaminated solution is presented in Tab. 1. The test power supply and device are depicted in Fig. 3.

Tab. 1 Contamination ratio table

NO.	1	2	3	4	5
ρ_{ESDD}/(mg•cm^2)	0.05	0.10	0.15	0.20	0.25
ρ_{NSDD}/(mg•cm^2)	0.50	1.00	1.50	2.00	2.50

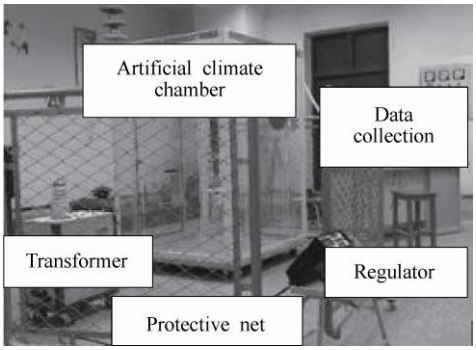

Fig. 3 Power supply and device for the test

2.3 Test methods

The insulator sample was stained using the quantitative coating method recommended by IEC60507 and GB/T4585 [12-13], First, the surface of the sample was cleaned using absolute ethanol, following which the sample was rinsed using large amount of deionized water to form a large-area water film on its surface, indicating that it was rinsed clean. Subsequently, it was placed in a dust-free environment to allow it to dry sufficiently. Subsequently, the insulator's surface area was calculated to find the required quantity of a solution containing sodium chloride (NaCl) and diatomaceous earth. The solution was then mixed well before applying uniformly on the surface of the test insulator. The insulator was then placed in a shaded cool place for 24 hours to dry naturally. Finally, after the drying, the sample insulator was hung inside the artificial climate chamber.

The test pressurization method, which employs a uniform extensor procedure, was used to better understand the change in flashover characteristics [7, 14]. Five to six flashover tests were performed on each of the three samples. All the flashover voltages were considered with an average error of up to 10%. The average value of the flashover voltage was taken as the average flashover voltage of the sample. The calculation formula of the flashover voltage U_f and its standard deviation σ is.

$$\begin{cases} U_f = \sum_{i=1}^{M} \dfrac{U_i}{M} \\ \delta = \sqrt{\dfrac{\sum_{i=1}^{M} (U_i - U_f)^2}{M-1}} \times \dfrac{100\%}{U_f} \end{cases} \tag{1}$$

where U_i denotes the flashover voltage obtained for each test, M the total number of tests performed, U_f the flashover voltage, and δ the standard deviation.

3 Test results and analysis

3.1 Effect of fog-water salt density on the flashover voltage of the samples

Composite insulator string FQBG-25, under various salt densities of the fog water, and the flashover voltage U_f with the changes in ρ_{ESDD} are presented in Tab. 2. Eq. 2 shows the fitting result of the pollution flashover voltage U_f with ρ_{ESDD} [15-18]. Furthermore, the fitting coefficients A and a, and the fitting variance R^2 during the fitting process are presented in Tab. 3. We have

$$U_f = A\rho_{ESDD}^{-a} \tag{2}$$

where U_f denotes the flashover voltage in kV, A denotes coefficients related to the shape of the insulator and the degree of contamination, ρ_{ESDD} the equivalent salt density in mg/cm^2, and a the characteristic index of ρ_{ESDD} on fouling U_f.

Tab. 2 FQBG-25 pollution flash voltage under different salt densities and fog water conductivities

ρ_{ESDD} (mg/cm^2)	Pollution flash voltage (kV)				
	σ = 0.002 S/m	σ = 0.01 S/m	σ = 0.1 S/m	σ = 0.3 S/m	σ = 0.5 S/m
0.05	53.672	51.528	48.895	44.038	39.310
0.10	46.287	44.434	42.156	38.259	34.715
0.15	42.799	41.360	39.347	35.752	32.294
0.20	40.162	39.185	37.340	33.961	31.330
0.25	38.569	37.698	35.974	32.860	31.109

Tab. 3 FQBG-25 pollution flash voltage under different salt densities and fog water conductivities

Fog conductivity/(S·m^{-1})	A		R^2
0.002	28.88	0.206 4	0.999 6
0.01	28.60	0.195 2	0.997 9
0.10	27.39	0.191 8	0.997 0
0.30	25.28	0.183 9	0.997 2
0.50	24.53	0.154 5	0.976 6

According to the analyses in Tab. 2 and Tab. 3, the following can be known.

(1) Under the condition that the ρ_{ESDD} of the surface of FQBG-25 is constant, U_f will decrease correspondingly upon increasing σ. As shown in Tab. 2, when ρ_{ESDD} is 0.10 mg/cm^2, σ changes from 0.002 to 0.50 S/m, and U_f drops from 46.287 to 34.715 kV. Moreover, when ρ_{ESDD} equals 0.10 mg/cm^2 and σ equals 0.002 S/m, the percentages of drop in the pollution flash voltage under the above-mentioned five cases of conductivity fogs are 0%, 4.00%, 8.92%, 17.34%, and 25%, respectively. When ρ_{ESDD} is 0.25 mg/cm^2, upon changing σ from 0.002 to 0.50 S/m, U_f drops from 38.569 to 31.109 kV. Furthermore, for ρ_{ESDD} equals to 0.25 mg/cm^2 and σ equals to 0.002 S/m, the percentages of drop in the pollution flash voltage under the five cases of conductivity fogs are 0%,

2.26%, 6.73%, 14.80%, and 19.34%, respectively.

(2) The flashover voltage in the presence of salty fog has dropped significantly, should consider the influence of the conductivity of the fog, thus introducing the concept of additional salt density. The effect of conductivity is completely equivalent to the additional salt density. As shown in Tab. 2, under the condition that ρ_{ESDD} is 0.10 mg/cm^2, the flashover voltage U_f values for σ equal to 0.002 S/m and under the index a, which characterizes the flashover voltage, are 46.287 and 0.206 4 kV, respectively. However, the values of U_f when σ is 0.50 S/m and under the index a are 34.715 and 0.154 5 kV, respectively.

(3) The formula for the flashover voltage in Eq. (2) is obtained under the condition of surface contamination only, to more accurately express the influence of the additional salt density of the fog-conductivity equivalent on the pollution flashover voltage. Furthermore, an additional salt-density coefficient K is introduced to correct the classical pollution flash voltage formula, which is corrected in Eq. (3). The corrected pollution flash voltage expression accurately expresses the result of the combination of high-conductivity salty fog and contamination on the surface of the insulator. We have

$$U_f = A(K\rho_{ESDD})^{-a} \tag{3}$$

To keep A and a unchanged for the case when fog-water conductivity is 0.002 S/m (clean fog), for U_f in Tab. 2, ρ_{ESDD} is obtained from the classical formula. This time, ρ_{ESDD} is recorded as the equivalent salt density value ρ^*_{ESDD}, which is the equivalent salt density when the fog water and the pollution co-exist. We then determined the additional salt density coefficient $K=\rho^*_{ESDD}/\rho_{ESDD}$. The specific coefficients are presented in Tab. 4.

Tab. 4 Correction factor K for different salt densities and fog water conductivities

ρ_{ESDD}/(mg/cm^2)	Correction factor K				
	σ=0.002 S/m	σ=0.01 S/m	σ=0.1 S/m	σ=0.3 S/m	σ=0.5 S/m
0.05	0.99	1.21	1.56	2.59	4.49
0.10	1.02	1.24	1.60	2.56	4.10
0.15	0.99	1.17	1.49	2.37	3.88
0.20	1.01	1.14	1.44	2.28	3.37
0.25	0.98	1.10	1.38	2.14	2.79

3.2 Effect of fog-water conductivity on sample flashover voltage

(1) The effect of high-conductivity fog on the flashover voltage of the insulator can be finally analyzed using additional salt density. The mist wets the surface of the insulator, indirectly changing the ρ_{ESDD} of the surface of the insulator. The equivalent salt density then becomes $K\rho_{ESDD}$, thereby lowering the flashover voltage.

(2) As can be seen from Fig. 4, the high-conductivity fog has a more obvious effect on the pollution voltage under the conditions of lower salt density and pollution. Furthermore, as shown in Tab. 2: a) When ρ_{ESDD} is 0.05 mg/cm^2, σ changes from 0.002 to 0.50 S/m, and U_f decreases by 26.76% from 53.672 to 39.310 kV; b) When ρ_{ESDD} is 0.15 mg/cm^2, σ changes from 0.002 to 0.50 S/m, and U_f decreases by 24.54% from 42.799 to 32.294 kV; c) When ρ_{ESDD} is 0.25 mg/cm^2, σ changes from 0.002 to 0.50 S/m, and U_f decreases by 19.34% from 38.569 to 31.109 kV.

(3) As the conductivity of the mist water continues to increase, the rate of decline of U_f increases. As shown in Tab. 2: a) When ρ_{ESDD} is 0.10 mg/cm^2, σ changes from 0.002 to 0.10 S/m, and U_f decreases by 8.92% from 46.287 to 42.156 kV; when σ changes from 0.10 to 0.50 S/m, and U_f decreases by 17.65% from 42.156 to 34.715 kV; b) When ρ_{ESDD} is 0.20 mg/cm^2, σ changes from 0.002 to 0.10 S/m, and U_f decreases by 7.03% from 40.162 to 37.340 kV; when σ changes from 0.10 to 0.50 S/m, U_f decreases by 16.10% from 37.340 to 31.330 kV.

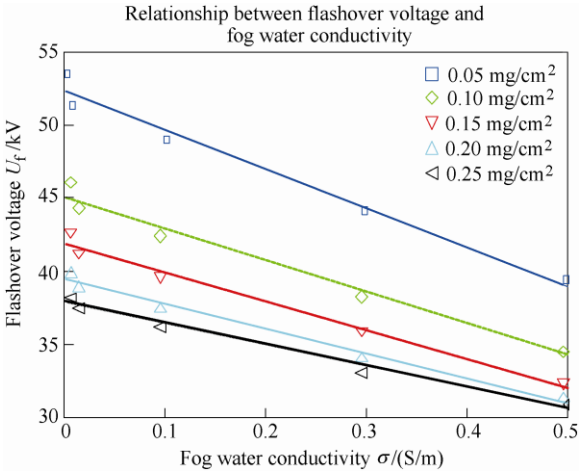

Fig. 4 Relationship between flashover voltage and fog-water conductivity at various equivalent salt deposit densities

4 Analysis of flashover characteristics under simulation

According to the previous test results, in the foggy water environment, the fog water will re-wet the dirty layer on the surface of the insulator, thereby increasing the equivalent salt value of the fouling layer on the surface, which, in turn, causes the flashover to occur more easily. To study the mechanism of flashover more profoundly, COMSOL Multiphysics, a multi-physics coupling software, is used to calculate the potential and electric-field strength of the charged contamination insulator in the salty fog according to the specific conditions (Tab.5), and to analyze the changes in the potential and electric-field strength. We further study the influence of the distribution of both potential and electric field on flashover voltage.

Tab. 5 Simulation parameter setting

Medium	ε_r	σ/(S·m^{-1})
Gold fittings	10^{10}	10^{-7}
Mandrel	6	10^{-12}
Jacket	3.5	10^{-13}
Contaminated water film	81	0.6-2.5
High conductivity fog	1.008	0.1-0.7

Because the wavelength of the power frequency alternating current is much larger than the structural length of the insulator, the electric field can be considered stable at any instant; therefore, the simulation analysis uses the electrostatic-field finite element method [19-20].

The simulation, however, ignores the non-axisymmetric part of the two ends of the insulator and establishes a simplified model. The resulting full-scale potential of the insulator and the 1/360 simplified model potential of the 1° center angle of the center axis are depicted in Fig. 5. The full-scale potential of the space and the 1/360 simplified model electric-field distribution of the 1° center angle of the center axis is depicted in Fig. 6. From Fig. 5 and Fig. 6, it can be concluded that the voltages of different parts of the insulator are greatly different, and that the electric-field strength is not the same. Larger value of electric-field strength is observed in the shed and the mandrel, and the maximum electric-field strength is observed at the junction of metal and silicone rubber. For a more accurate analysis, this article further

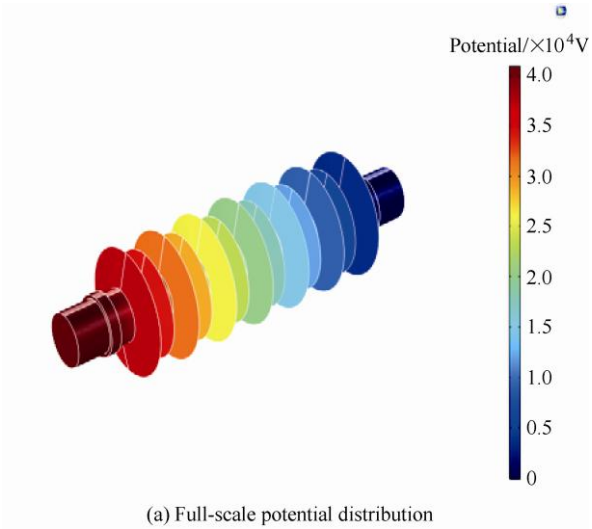

(a) Full-scale potential distribution

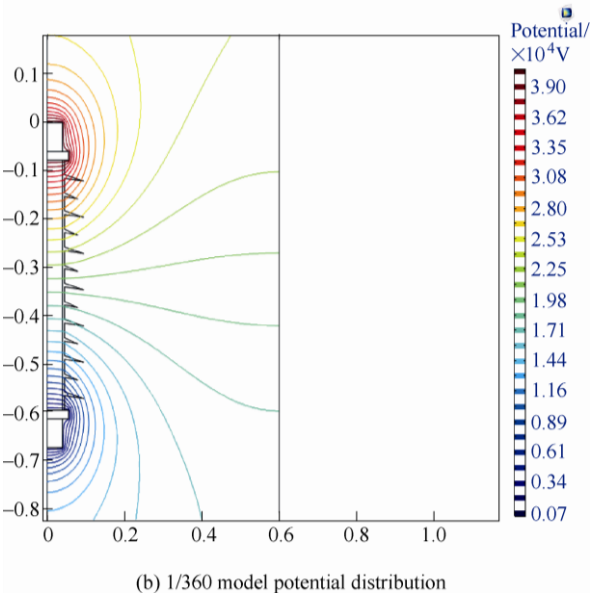

(b) 1/360 model potential distribution

Fig. 5 Potential distribution

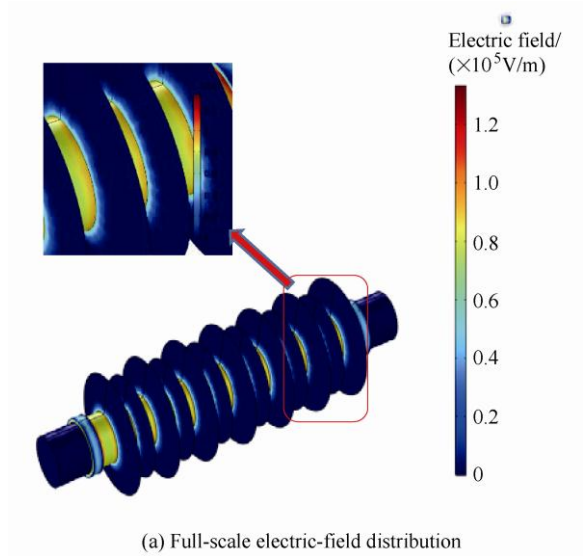

(a) Full-scale electric-field distribution

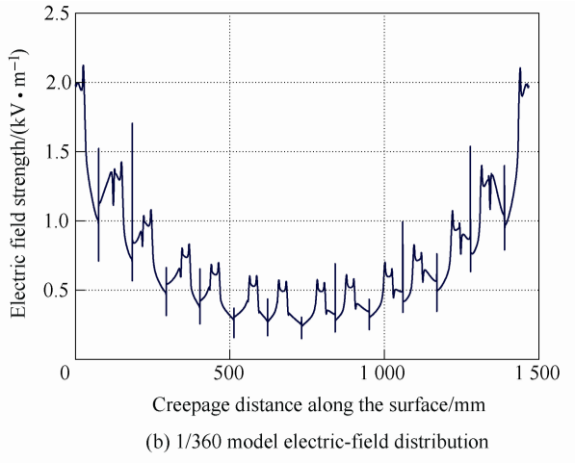

(b) 1/360 model electric-field distribution

Fig. 6 Electric-field distribution

extracts the potential and the electric field of a large small umbrella skirt from the low-voltage end fittings and compares the potential and the electric field results of different fog-water conductivities under the same equivalent salt density, as depicted in Fig. 7. The results of the potential and electric field under different equivalent salt densities for the same fog-water conductivity are also compared, as depicted in Fig. 8.

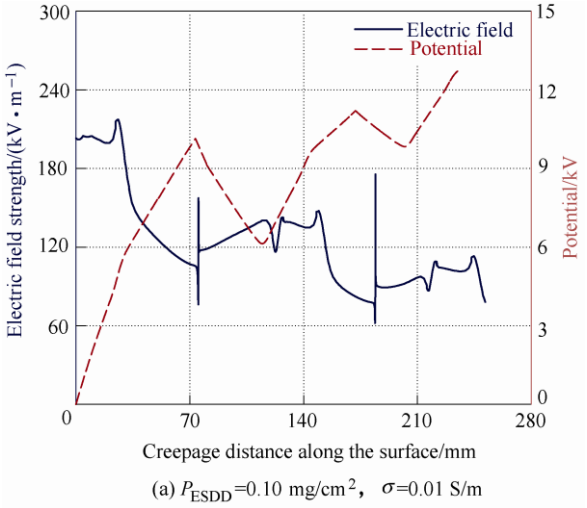

(a) P_{ESDD}=0.10 mg/cm^2, σ=0.01 S/m

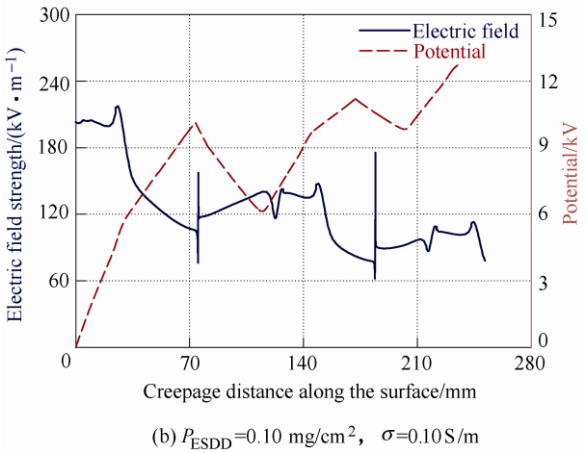

(b) P_{ESDD}=0.10 mg/cm^2, σ=0.10 S/m

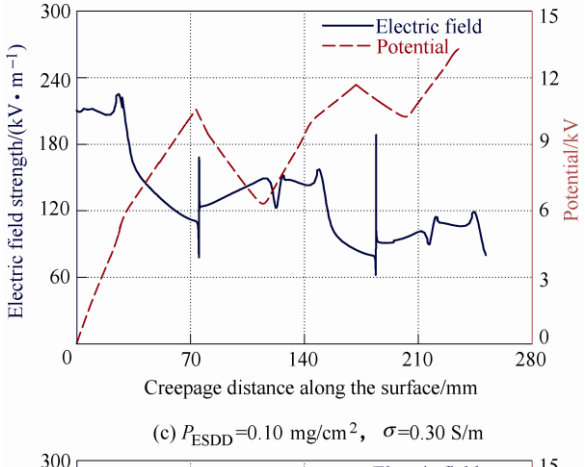

(c) P_{ESDD}=0.10 mg/cm^2, σ=0.30 S/m

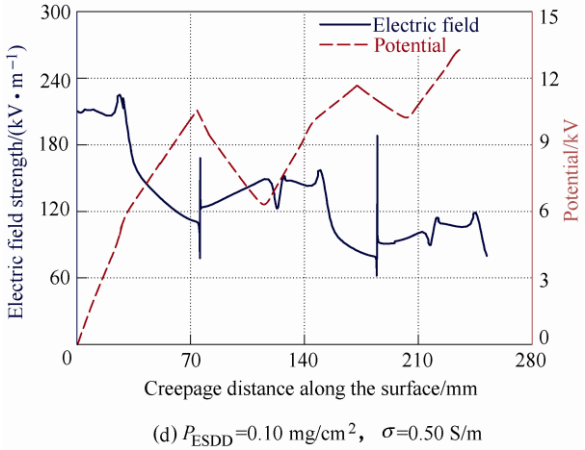

(d) P_{ESDD}=0.10 mg/cm^2, σ=0.50 S/m

Fig. 7 Surface potential and electric-field distribution of insulators under different fog-water conductivities

Fig. 7 depicts the distribution of both the potential and the electric field when ρ_{ESDD} is constant at 0.10 mg/cm^2, where σ is 0.01, 0.10, 0.30, and 0.50 S/m, respectively, in Fig. 7a, Fig. 7b, Fig. 7c, and Fig. 7d. It can be seen from the simulation results that when σ is 0.01, 0.10, 0.30, and 0.50 S/m, the maximum increase in the potential is 2.41%, 2.45%, 2.52%, and 2.67%, respectively; moreover, the maximum increase in the electric-field strength is 2.78%, 3.31%, 4.68%, and 4.93%, respectively.

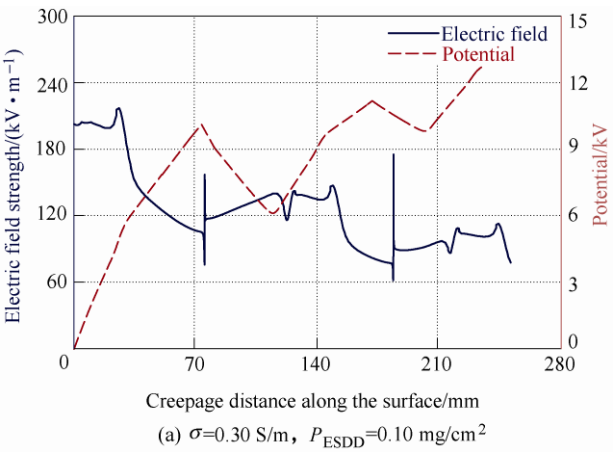

(a) σ=0.30 S/m, P_{ESDD}=0.10 mg/cm^2

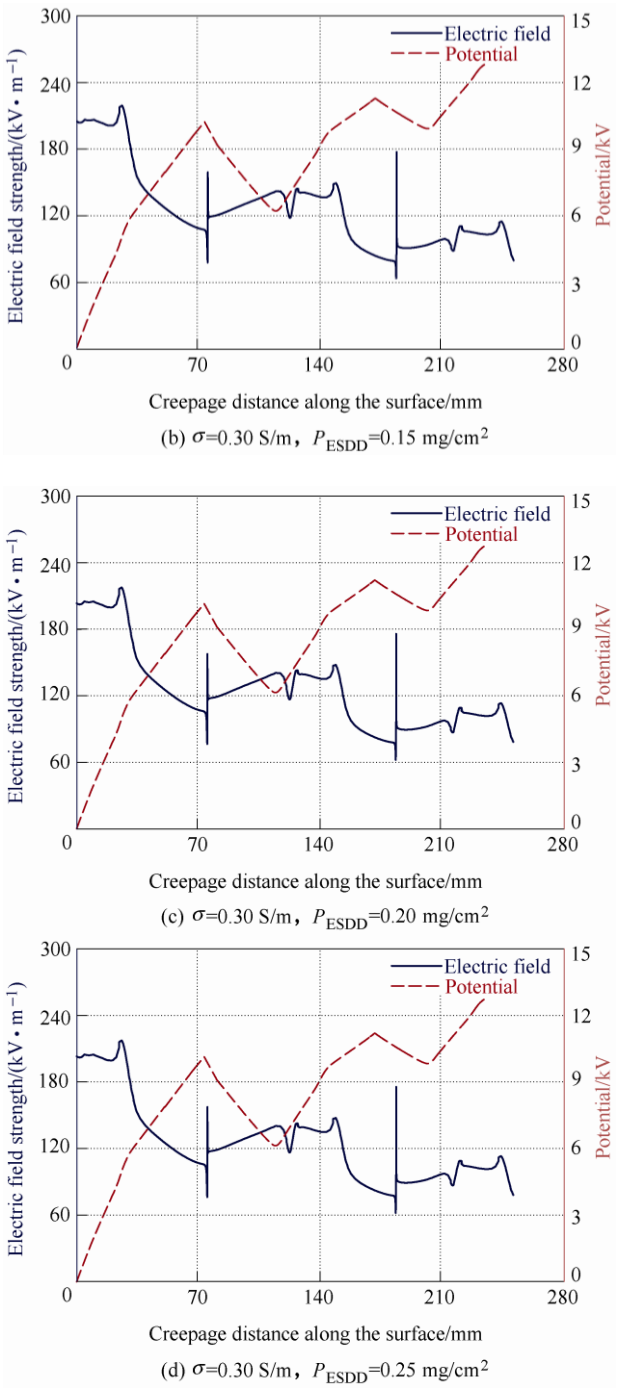

Fig. 8 Surface-potential and electric-field distribution of insulators under different salt densities

Fig. 8 depicts the distribution of both the potential and the electric field when σ is constant at 0.30 S/m, the salt density of the insulator surface is 0.10, 0.15, 0.20, and 0.25 mg/cm^2, respectively, in Fig. 8a, Fig. 8b, Fig. 8c and Fig. 8d.. It can be observed from the simulation results that when ρ_{ESDD} is 0.10, 0.15, 0.20, and 0.25 mg/cm^2, the maximum potential increase is 2.52%, 2.44%, 2.27%, and 2.06%, respectively. Furthermore, the maximum increase in the electric-field strength is 4.87%, 4.62%, 4.59%, and 4.35%, respectively.

By calculating the electric field and potential of the surface of the insulator under different fog salt densities, the simulation results, combined with the experimental results from the test, show that the electric-field changes are obvious, and that the high-conductivity fog water affects the contamination layer on the surface of the insulator, which, in turn, affects the flashover voltage, electric-field strength, and potential. Therefore, the results from the test are better proved by the simulation results.

5 Conclusions

(1) The salty fog will affect the pollution flashover voltage of the insulators. The specific salt density correction coefficient K, which provides a theoretical basis for the selection and optimization of the wrist insulators of the railway OCS in the saline-alkali area, is obtained.

(2) The flashover voltage of the FQBG-25 long rod type wrist arm composite railway-specific insulator will decrease with the increase in fog-water conductivity; as the conductivity of the fog water continues to increase, the rate of decline of the flashover voltage will also increase.

(3) The specific additional salt density coefficient is obtained; the smaller the salt density value of the original insulator surface, the larger is the additional salt density coefficient, and the more obvious is the effect on the flashover characteristics.

(4) The conductivity of the salty fog affects the distribution of both the potential and the electric field on the surface of the insulator, but the effect on the electric-field strength is greater than that on the potential. The equivalent salt density of the fouling layer and the increase in the electric-field strength together lead to a decrease in the flashover voltage, but the former has a more significant effect on the reduction of the flashover voltage.

References

[1] Wang Feng, Li Zhuo, Zhang Yingli, et al. PIC/MCC simulation of the dynamic process of surface charge accumulation on composite insulators. *High Voltage Engineering*, 2015, 41(8): 2750-2756.

[2] Meng Zhigao, Jing Xingliang, Dong Bingbing, et al. AC

pollution flashover characteristics of surged polluted glass and composite insulators under natural fog conditions. *Transactions of China Electrotechnical Society*, 2016, 31(12): 65-71.

[3] Wang Liming, Liang Jianyu, Dai Hanqi, et al. Influence of high conductivity fog on the hydrophobicity of composite insulator . *Power System Technology*, 2014, 38(7): 1779-1785.

[4] X Jiang, Y Guo, Z Meng, et al. Additional salt deposit density of polluted insulators in salt fog. *IET Generation Transmission & Distribution*, 2016, 10(15): 3691-3697.

[5] K Wang, C Zhao, M Zhu, et al. Analysis on flashover performance of polluted porcelain insulators in high conductivity fog environment. *Electrical Insulation and Dielectric Phenomena*, IEEE, 2015: 193-196.

[6] Geng Jianghai, Zhong Zheng, Liu Yunpeng, et al. Effect of high conductivity fog on AC flashover characteristics of suspended porcelain insulators. *High Voltage Engineering*, 2017, 43(9): 2976-2982.

[7] Zhang Zhijin, Li Chen, Liang Tian, et al. Effect of charged salt spray environment on flashover characteristics of composite insulator silicone rubber. *Power System Technology*, 2018, 42(7): 2153-2159.

[8] Liu Changyi, Wang Liming, Liu Dong, et al. Influence of fog-haze parameters on equivalent salt deposit density of external insulation. *High Voltage Engineering*, 2016, 42(6): 1841-1847.

[9] Xu Feng, Niu Shengjie, Zhang Yu, et al. Analyses on chemical characteristic of spring sea fog water on Donghai island in Zhanjiang, China. *China Environmental Science*, 2011, 31(3): 353-360.

[10] Xu Sen, Wu Chao, Li Tao, et al. Research on pollution accumulation characteristics of insulators during fog-haze days. *Proceedings of the CSEE*, 2017, 37(7): 2142-2150.

[11] Zhang Hu, Huang Daochun, Xu Tao, et al. Study on the correction of AC pollution withstand voltage of disc-shaped suspension insulators considering $CaSO_4$. *Chinese Journal of Electrical Engineering*, 2016, 36 (6): 1739-1747.

[12] China Electrical Equipment Industry Association. GB/T 4585—2004 Artifical pollution test on high-voltage insulators to be used on A.C. systems. Beijing:Standards Press of China, 2004.

[13] IEC 60507 Artificial pollution test on high-voltage insulators to be used on AC systems. Geneva:International Electrotechnical Commission, 1991.

[14] Jiang Xingliang, Xiao Daibo, Hu Jianlin, et al. Influence of test methods on pollution flashover performance of composite insulators [J]. *High Voltage Apparatus*, 2010, 46(2): 8-11.

[15] G N Ramos, M T Campillo, R K Naito. A study on the characteristics of various conductive contaminants accumulated on high voltage insulators. *IEEE Transactions on Power Delivery*, 1993, 8(4): 1842-1850.

[16] R Matsuoka, K Kondo. Influence of nonsoluble contaminants on the flashover voltages of artificially contaminated insulators. *IEEE Transactions on Power Delivery*, 1996, 11(1): 420-430.

[17] Zhang Zhijin, Jiang Xingliang, Sun Caixin. Research status and prospects of flashover characteristics of polluted insulators. *Power System Technology*, 2006, 30(2): 35-40.

[18] A Mekhaldi. Flashover of discontinuous pollution layer on HV insulators. *IEEE Transactions on Dielectrics and Electrical Insulation,* 1999, 6(6): 900-906.

[19] Zhang Youpeng, Zhao Shanpeng, Chen Zhigong, et al. Effect of suspended sand on potential and electric field distribution of rod insulator. *High Voltage Engineering*, 2014, 40(9): 2706-2713.

[20] Xu Zhiniu, Lü Fangcheng, Li Heming, et al. Influencing factors of insulator electric field analysis by finite element method and its optimization. *High Voltage Engineering*, 2011, 37(4): 944-951.

Sihua Wang was born in Jiangsu Province, China, on May 21, 1968. He graduated in electrical engineering and automation from the East China Jiaotong University, Jiangxi, China, in 1995. He is a professor at Lanzhou Jiaotong University, Lanzhou, China.

His research interests concern: Reliability of Substation Integrated Automation and Direction of HV Insulation.

Youlong Wu was born in Gansu Province, China, on June 16, 1991. He is studying for a master's degree in electrical engineering at the Lanzhou Jiaotong University, Lanzhou, China.

His research interest concerns high voltage and insulation technology.